

Discovery and Timing of the First Millisecond Pulsar in NGC 6316

D. BHAKTA ^{1,2}, S. RANSOM ², M. DECESAR ³ AND S. DAI ^{4,5}

¹*Department of Astronomy, University of Virginia, 530 McCormick Road, Charlottesville, VA 22904, USA*

²*National Radio Astronomy Observatory, 520 Edgemont Road, Charlottesville, VA 22903, USA*

³*College of Science, George Mason University, Fairfax, VA 22030, USA*

⁴*Australia Telescope National Facility, CSIRO, Space and Astronomy, PO Box 76, Epping, NSW 1710, Australia*

⁵*Western Sydney University, Locked Bag 1797, Penrith South DC, NSW 2751, Australia*

ABSTRACT

NGC 6316 is a poorly studied, distant, and massive globular cluster (GC) with prominent gamma-ray emission detected via the *Fermi* Large Area Telescope (LAT). Based on gamma-ray spectral studies, NGC 6316 is expected to host tens of millisecond pulsars (MSPs). Using the Green Bank Telescope (GBT) and Murriyang, CSIRO's Parkes radio telescope (Parkes), we present the discovery and a 3.1 yr duration timing solution of the first millisecond pulsar found in the cluster. PSR J1716–2808A has a rotational period of 2.45 ms and is in a binary with a $\sim 0.1 M_{\odot}$ companion with an orbital period of 0.42 d. This is a normal-looking MSP within a compact orbit with no evidence of eclipses. PSR J1716–2808A has a dispersion measure $DM = 172.26 \text{ pc cm}^{-3}$, which is lower than predicted NE2001 and YMW16 electron density model values. The MSP is located within half a core radius from the cluster center and has a negative period derivative, implying that it is on the back side of the cluster and is being accelerated towards us. Given the negative period derivative, we report an upper limit on the maximum line-of-sight cluster acceleration, $a_{l,\text{max}}/c \approx 2.3 \times 10^{-18} \text{ s}^{-1}$, experienced by the pulsar and constraints on the magnetic field to be $< \sim 3 \times 10^8 \text{ G}$. This confirms the pulsar to be within NGC 6316 despite the lower-than-expected dispersion measure. We can better constrain NGC 6316's properties through longer-term timing of PSR J1716–2808A or by finding more pulsars within the cluster. Based on the gamma-ray pulsar estimates and a cluster distance of 11.3 kpc, deeper, more sensitive searches would find many additional pulsars.

Keywords: Millisecond pulsars (1062) — Binary pulsars (153) — Globular star clusters (656)

1. INTRODUCTION

Millisecond pulsars are created preferentially in globular clusters (GCs) when compared, per unit stellar mass, to the Galactic disk. In contrast with pulsars in the Galactic field, of which $\sim 10\%$ are in binary systems (R. N. Manchester et al. 2005)⁶, more than 50% of all known GC pulsars are in binary systems⁷. This is due to the large stellar density and the resulting interactions that occur within the clusters (A. S. Fruchter & W. M. Goss 2000; F. Verbunt & P. C. C. Freire 2014; E. S. Phinney 1993; W. Wu et al. 2021). Searching for and conducting long-term timing of these MSPs can yield significant insight into these GCs. Multiple cluster MSPs can

be timed to constrain and model the cluster's ionized gas content (S. M. Ransom 2008; C. S. Ye et al. 2019). Short-period eclipsing binaries can provide information on pulsar winds, and the nature of the companion stars (P. C. C. Freire 2005). Furthermore, binary parameters can be measured and used to study binary evolution, and subsequent NS mass measurements can constrain the nuclear equation of state (C. M. Zhang et al. 2011; F. Özel & P. Freire 2016; H. T. Cromartie et al. 2020). The period derivatives and position measurements of these cluster pulsars can provide measurements on the host cluster's mass distribution and dynamics due to the period derivatives being dominated by gravitational accelerations from the cluster (E. S. Phinney 1993; S. M. Ransom 2008; B. J. Prager et al. 2017).

Fermi-LAT has detected GCs in γ rays (A. A. Abdo et al. 2009, 2010; S. Abdollahi et al. 2020; D. Song et al. 2021; P. C. C. Freire et al. 2011; J. H. K. Wu et al. 2013). It is likely that MSPs are the dominant sources of γ -

Corresponding author: D. Bhakta

Email: drb7tg@virginia.edu

⁶ <http://www.atnf.csiro.au/research/pulsar/psrcat>

⁷ See <https://www3.mpifr-bonn.mpg.de/staff/pfreire/GCpsr.html> for a list ++of all known GC pulsars

ray emission within GCs (A. A. Abdo et al. 2009, 2010; S. Abdollahi et al. 2020; D. Song et al. 2021; P. C. C. Freire et al. 2011; J. H. K. Wu et al. 2013). Gamma-ray pulsations from MSPs within several clusters have been detected, albeit rare; only 3 GC MSPs have been confirmed as γ -ray MSPs (P. C. C. Freire et al. 2011; J. H. K. Wu et al. 2013; P. Zhang et al. 2022), likely due to high background and galactic confusion. Estimates based off of the γ -ray spectral properties indicate tens of pulsars should populate several of the brightest clusters (R. de Menezes et al. 2019; W. Wu et al. 2021), including NGC 6316.

NGC 6316 is a scarcely investigated massive ($M \sim 3.5 \times 10^5 M_{\odot}$, top 20% of GCs) bulge cluster located approximately 11.3 kpc (D. Deras et al. 2023) from the Sun (H. Baumgardt et al. 2019). T. J. Davidge et al. (1992) and more recently, D. Deras et al. (2023) noted similarities between NGC 6316 and 47 Tuc based on their color-magnitude diagrams and age. 47 Tuc currently has 42 known pulsars within the cluster (behind Terzan 5’s 49 pulsars)⁸. Studies of the γ -ray emission predict anywhere from 13 MSPs (W. Wu et al. 2021) to 10^2 MSPs (R. de Menezes et al. 2019) within NGC 6316. We have conducted radio searches of NGC 6316 alongside several other γ -ray bright globular clusters to search for new MSPs. As a part of this search, we have observed the GCs: NGC 6304, NGC 6717, NGC 6139, NGC 6388, GLIMPSE-C02, 2MASS-GC01, Terzan 2, and Liller 1, with data reduction and searches on-going for the other clusters. In this paper, we report the discovery and timing of a highly accelerated MSP within a compact binary system in NGC 6316.

2. GBT OBSERVATIONS

We observed NGC 6316 with the Robert C. Byrd Green Bank Telescope (GBT; R. M. Prestage et al. (2009)) using the C–band and S–band receivers, and observed late August 2022 and late December 2022 respectively (project ID: AGBT22B_270, PI: D. Bhakta). The observation parameters are listed in Table. 1.

We used PRESTO⁹ (S. Ransom 2011) to search for periodic pulsations in the GBT S–band and C–band data with `rfifind` to mask and zap radio-frequency interference. We dedispersed the data into barycentric time series ranging $0\text{--}471 \text{ pc cm}^{-3}$ using `prepsubband` and `DDplan.py` with 471 pc cm^{-3} selected as the max predicted DM via the NE2001 and YMW16 electron density models (371 pc cm^{-3}) + 100 pc cm^{-3} to account for uncertainties in DM estimates (J. M. Cordes & T. J. W.

Lazio 2002; J. M. Yao et al. 2017). In order to search for short orbital period pulsars, we searched the observations in 30–45 minute durations in addition to the full 2 hr duration. We used the routine `accelsearch` to search for periodic signals in the Fourier domain, with $z_{max} = 10, 200$ and 600 for the full duration and $z_{max} = 200$ for the shorter duration searches. z_{max} represents the maximum number of Fourier frequency bins that a signal can drift during an individual observation due to a pulsar’s acceleration (S. M. Ransom et al. 2002). Using `ACCEL_sift.py`, we filtered and identified candidates for folding with `prepfold` within PRESTO.

3. PSR J1716–2808A DETECTION

We identified a highly accelerated pulsar candidate in the $z_{max} = 600$ full duration search ($z = 146.0$ corresponding to an acceleration of 2.7 ms^{-2}) with a spin period $P \simeq 2.45 \text{ ms}$ at $\text{DM} \simeq 172 \text{ pc cm}^{-3}$ in the second S–band observation (coherently dedispersed at $\text{DM} 281.5 \text{ pc cm}^{-3}$) on MJD 59945. Due to the highly accelerated nature of the candidate, we searched over \ddot{P} with `prepfold` in order to fold the new MSP through the full observation shown in Fig 1. We detected the new MSP, PSR J1716–2808A in the incoherently dedispersed S–band observation from MJD 59939 but not the C–band observations. The large acceleration indicated that this MSP is in a compact binary. We conducted a DDT observation with Murriyang, CSIRO’s Parkes radio telescope (hereafter “Parkes”) to check if the MSP is detectable with the Parkes ultra-wide-bandwidth, low frequency receiver (UWL) (G. Hobbs et al. 2020) before following up with a dedicated timing campaign.

3.1. Parkes Timing

Our Parkes DDT observation occurred on MJD 60282 for 3.5 hrs. The observing setup used the MEDUSA backend with 3328 MHz observing band across 26 subbands (128 MHz per subband), 64 μs sampling, and coherent dedispersion at $\text{DM} 172.00 \text{ pc cm}^{-3}$ in search mode. We processed and analyzed the data identically to the GBT observations with no detection using acceleration searches over the full observation as well as with short duration searches. Given the two S–band detections, we created a family of circular orbital solutions using `fit_circular_orbit.py` from PRESTO. These possible orbits were applied to topocentric timeseries generated at the DM of the S–band detections to search for a detection using `SPIDER_TWISTER`¹⁰.

⁸ <https://www3.mpifr-bonn.mpg.de/staff/pfreire/GCpsr.html>

⁹ <http://www.cv.nrao.edu/~sransom/presto/>

¹⁰ https://alex88ridolfi.altervista.org/pagine/pulsar_software_SPIDER_TWISTER.html

Observatory	Receiver	Dedispersion	f_{cent}	Δf	T_{obs} (# x hr)	T_{int} (μ s)	N_{chan}	N_{pol}
GBT	C-band	Incoherent	6011	4500	2x2	43.69	1024	1
GBT	S-band	Incoherent	2165	1500	1x2	10.92	1024	1
GBT ^a	S-band	Coherent: 281.5	2165	1500	1x2	43.69	1024	1
Parkes	UWL	Coherent: 172	2368	3328	9x3, 9x3.5	64	3328	1
GBT	L-band	Coherent: 172	1500	800	2x5	10.24	512	4

Table 1. Observation set up parameters for all NGC 6316 observations. All data was recorded in 8-bit format ^a The initial detection of PSR J1716–2808A.

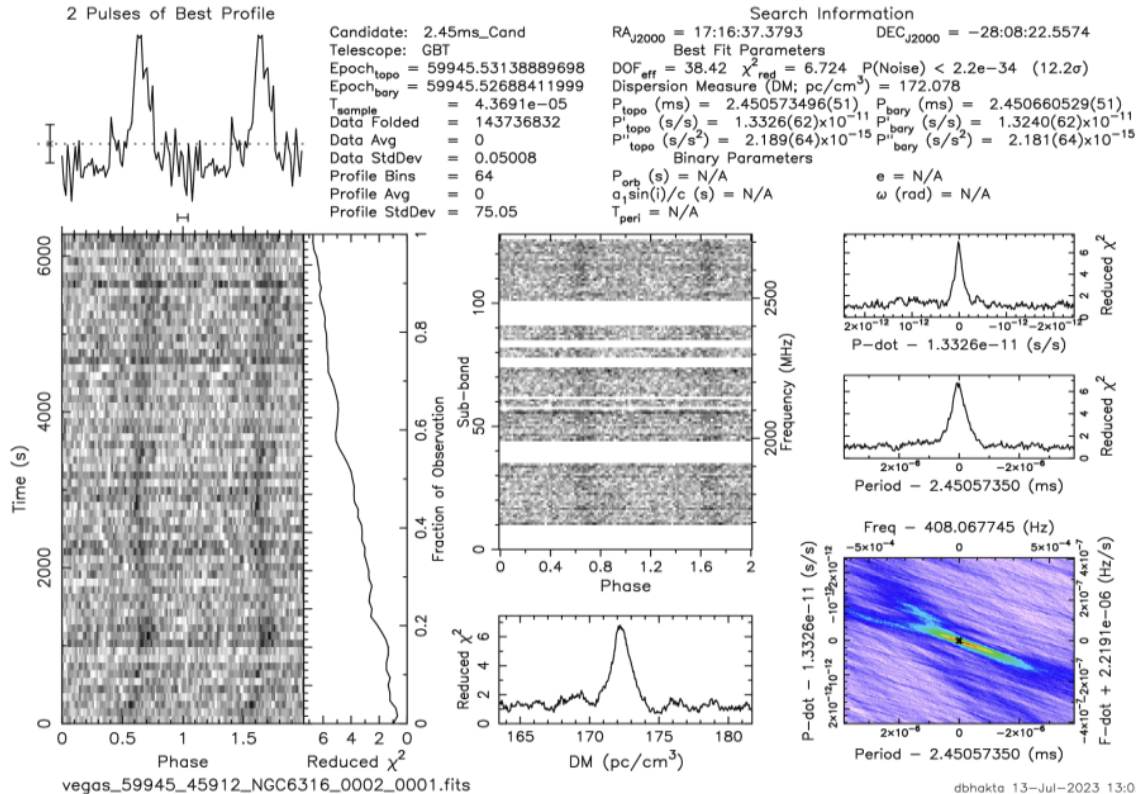


Figure 1. The `prepfold` output of the first detection of PSR J1716–2808A from a GBT S–band observation. The residual curvature in the time vs pulse phase greyscale on the left indicates uncorrected orbital motion despite fitting for acceleration and jerk (i.e. \dot{p} and \ddot{p}).

`SPIDER_TWISTER` folds the timeseries across many trials, where the time of passage at the ascending node (T_{asc}) is slightly altered to search over the orbital phase of a binary, and the highest signal-to-noise value is returned. Using `SPIDER_TWISTER`, we detected PSR J1716–2808A in the Parkes DDT observation. However, we were unable to further constrain the orbital solutions, as the Parkes detection overlapped with the previous detections in orbital phase. Given the successful detection with the Parkes DDT, we conducted a dedicated timing campaign using Parkes (project ID: P1330, PI: D. Bhakta) to fully solve the orbit of the binary and determine a phase-connected timing solution. Ad-

ditionally, we conducted 2×5 hr observations (observed on MJDs 60623 and 60650) with the GBT at L–band for deeper, more sensitive pulsation searches (project AGBT24B430, PI D. Bhakta) with the additional advantage of the longer observing tracks providing greater orbital coverage. With the new GBT and Parkes observations, we solved the orbit and phase-connect across a 3yr timing baseline.

4. RESULTS

Timing parameters of PSR J1716–2808A are reported in Table 2. We measured astrometric position, spin frequency and spin frequency derivative, and the Ke-

Table 2. Parameters for PSR J1716–2808A

Dataset and model summary	
Pulsar name	J1716–2808A
MJD range	59818–60946
Data span (yr)	3.09
Number of TOAs	135
Solar system ephemeris	DE440
Timescale	TT(BIPM2023)
PEPOCH, Spin Reference (d)	60623.685022
Time unit	TDB
Binary model	ELL1
Number of EFACs	5
Number of EQUADs	1
Measured Quantities	
Right Ascension (RA, J2000)	17 ^h 16 ^m 37 ^s .54045(19)
Declination (DEC, J2000)	–28° 08′ 22″.900(29)
Spin-frequency, f (Hz)	408.0317456967(1)
\dot{f} (Hz s ^{–1})	$1.396(5) \times 10^{-15}$
Dispersion measure (pc cm ^{–3})	172.265(8)
Orbital period (d)	0.424976623(2)
Projected semi-major axis (ls)	0.339253(4)
Time of ascending node (d)	59939.333399(4)
Fit Statistics	
Reduced chi-squared value	1.12
TOA residual (μ s)	30.94
Derived Quantities	
p , Spin-period (s)	0.0024507897009153(7)
\dot{p} , Spin-period derivative 1	$-8.37(3) \times 10^{-21}$
Eccentricity Upper Limit	7×10^{-5}
Mass Function (M_{\odot})	0.0002321251(87)
Min Companion Mass (M_{\odot})	≥ 0.08

plerian orbital parameters. An upper limit on the eccentricity for the circular orbit is $e < 7 \times 10^{-5}$, with the minimum companion mass of $\sim 0.1 M_{\odot}$. The pulsar position is $\sim 4.5''$ from the cluster center and within the cluster core ($r_{core} \sim 10''$) (D. Deras et al. 2023). PSR J1716–2808A’s dispersion measure is $172.26 \text{ pc cm}^{-3}$, which is lower than predicted values from the NE2001 ($DM \sim 191 \text{ pc cm}^{-3}$) and YMW16 ($DM \sim 371 \text{ pc cm}^{-3}$) electron density models (J. M. Cordes & T. J. W. Lazio 2002; J. M. Yao et al. 2017). Our TOAs show full orbital coverage with no evidence of eclipses, confirming that this is not a spider pulsar and appears to be a typical MSP in a highly accelerated, compact orbit binary system. Given the positive spin frequency derivative, the observed \dot{f} is likely dominated by accelerations within the cluster (E. S. Phinney 1992, 1993).

4.1. Contributions to observed Acceleration

The observed spin-down \dot{P}_{obs} is comprised of a combination of the intrinsic spin-down of the pulsar \dot{P}_{int} and several external accelerations, such as the Shklovskii effect (a_{PM} , i.e. the transverse Doppler effect from the pulsar’s proper motion) (I. S. Shklovskii 1970), the cluster potential acceleration (a_{GC}) (E. S. Phinney 1993), the galactic potential acceleration (a_G) (e.g. D. J. Nice & J. H. Taylor 1995), and acceleration due to nearby objects (a_{NN}) (S. Dai et al. 2023).

$$\left(\frac{\dot{P}}{P}\right)_{obs} = \left(\frac{\dot{P}}{P}\right)_{int} + \frac{a_{GC} + a_G + a_{PM} + a_{NN}}{c}. \quad (1)$$

Typically, the cluster acceleration a_{GC} dominates over the other terms, but without significant measurements on the binary non-Keplerian parameters (such as P_{orb}), we can only make order-of-magnitude estimates of the contributions of each acceleration term (P. C. C. Freire et al. 2017; B. J. Prager et al. 2017). We estimate the acceleration due to the galactic potential acceleration to be $a_G/c \approx 1.3 \times 10^{-18} \text{ s}^{-1}$, within a factor of ~ 2 using Eq. 3.5 from D. J. Nice & J. H. Taylor (1995), due to limitations in our knowledge of the Galactic potential, with R_0 and Θ_0 values reported in M. J. Reid et al. (2019) and cluster values from the Baumgardt catalog¹¹ (H. Baumgardt et al. 2019). For the Shklovskii effect (I. S. Shklovskii 1970), we estimate $a_{PM}/c \approx 6.0 \times 10^{-22} \text{ s}^{-1}$ and assuming that the pulsar has the same proper motion of the cluster. Lastly, we estimate $|a_{NN}/c| \approx 1.5 \times 10^{-19} \text{ s}^{-1}$ using Eq. 4 from S. Dai et al. (2023).

4.1.1. Acceleration Profiles

We derive an upper limit, $a_{l,max}/c \approx 2.3 \times 10^{-18} \text{ s}^{-1}$, on the cluster acceleration from \dot{P}_{obs}/P and assuming zero intrinsic spin-down,

$$a_{l,max} \doteq a_{l,GC} + \frac{\dot{P}_{int}}{P}c = \frac{\dot{P}_{obs}}{P}c - \mu^2 d - a_G - a_{NN}, \quad (2)$$

which is plotted in Fig. 2 as an inverted triangle for PSR J1716–2808A. The solid lines represent the predicted maximum line-of-sight acceleration due to the cluster potential ($a_{l,GC,max}$ calculated using two different models: Eq. 3.5 from E. S. Phinney (1993),

$$\frac{\max a_{GC}}{c} = \frac{3\sigma_v^2}{2c(r_c^2 + r_p^2)^{1/2}}, \quad (3)$$

and an analytical model using the mass distribution presented in I. King (1962) and described in P. C. C. Freire

¹¹ <https://people.smp.uq.edu.au/HolgerBaumgardt/globular/parameter.html>

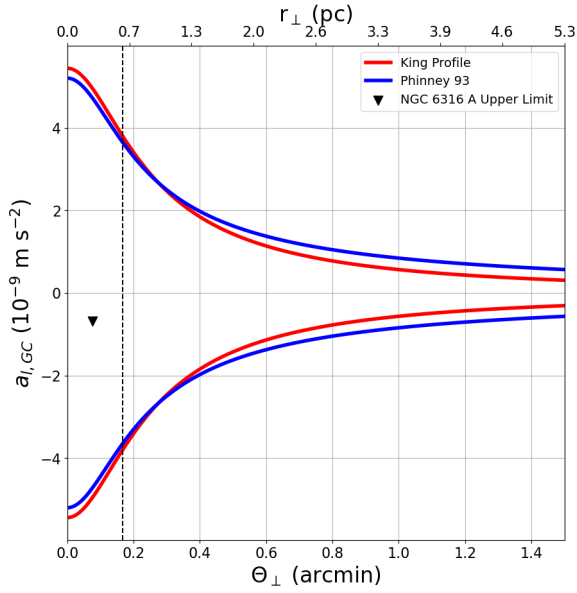


Figure 2. Maximum line of sight cluster acceleration profiles calculated using Eq. 3 and Eq. 4 as a function of the total angular offset from the center of NGC 6316. The dashed vertical line denotes the core radius. The upper limit for the cluster acceleration from PSR J1716–2808A, assuming zero intrinsic spin-down, is shown via the inverted triangle and calculated via Eq. 2. Given the estimated upper limit of PSR J1716–2808A, we cannot constrain properties of the cluster without either detecting more MSPs or by measuring the orbital period derivative of PSR J1716–2808A through continued timing.

et al. (2005),

$$a_{l,GC}(x) = \frac{9\sigma_z^2 l}{D\theta_c x^3} \left(\frac{x}{\sqrt{1+x^2}} - \sinh^{-1}x \right), \quad (4)$$

where σ_z is the 1D central velocity dispersion ($\sigma_z \approx 7.6$ km s⁻¹), θ_c is the core radius ($\theta_c \approx 10''$, D. Deras et al. 2023), D is the distance, l is the distance in core radii to the plane of the sky that passes through the center of the cluster, so that $x = \sqrt{l^2 + x_\perp^2}$, and $x_\perp = r_\perp/r_c$. We maximize the value of l at each r_\perp in order to calculate the maximum values of $a_{l,GC,max}$, shown via the red curve in Fig 2. In order to keep the predicted cluster acceleration as seen by the pulsar consistent with the maximum predicted lines (as shown in red and blue in Fig. 2), the pulsar’s magnetic field must be $< \sim 3 \times 10^8$ G.

4.2. Scattering and Flux Measurements

We used PSRCHIVE and our calibrated GBT L–band observations to measure PSR J1716–2808A’s flux density $S_{1.5\text{ GHz}} \approx 43 \pm 0.8 \mu\text{Jy}$. We detected no measurable polarization and therefore could not constrain the rotation measure (RM). We summed all the flux calibrated L–band observations using `psradd`, aligning the obser-

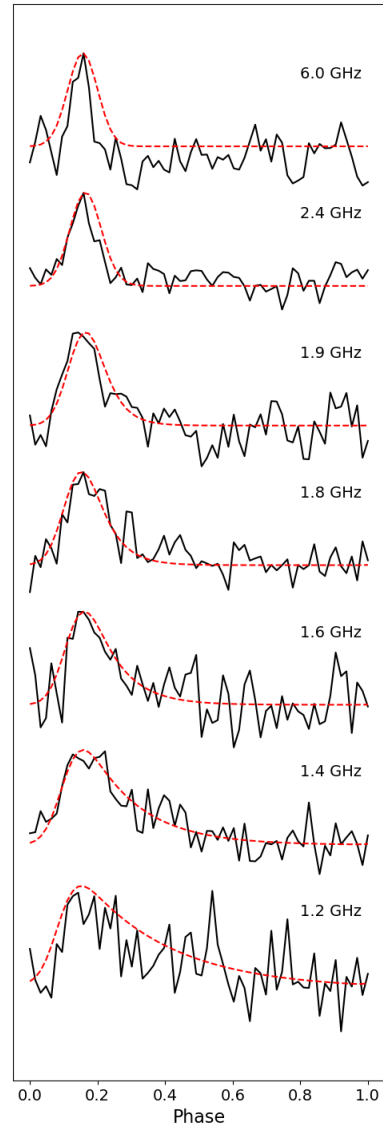


Figure 3. Estimated scattering profiles for the flux calibrated summed L–band subbands, uncalibrated S–band subbands and C–band observation. The normalized subbands are plotted in black and the estimated scattering profile is plotted in red with: $\tau_{1\text{ GHz}} \sim 1.4 \pm 0.1$ ms.

vations using the summed profile as a template (with the -P flag) in order to try to measure the pulse broadening from scattering across 6 subbands. We also co-added our uncalibrated Parkes UWL observations, using the same alignment procedure to increase signal to noise and measure scattering across 8 subbands. Additionally, we created subbanded profiles from the GBT S–band observations to measure scattering across the calibrated L–band and uncalibrated S–band observing bands. From the three approaches, we estimate the scattering to be roughly $\tau_{1\text{ GHz}} \sim 1.4 \pm 0.1$ ms from our various GBT and Parkes observations. We used the

$\tau_s \propto \nu^{-4}$ relation to scale the profiles to 1 GHz and convolved the profiles with a one-sided exponential function to estimate the scattering. Given the systematic uncertainties due to low signal-to-noise and only minimal scattering at these frequencies (see Fig. 3), the best way to more accurately measure the scattering would involve higher signal-to-noise observations with the new GBT Ultra-wideband Receiver (UWBR), which would also allow for more accurate flux density, spectral index, and potentially polarization measurements.

5. GAMMA RAY PULSATION SEARCH

We performed a search for gamma-ray pulsations from PSR J1716–2808A in the *Fermi*-LAT data. We selected Pass 8 SOURCE-class photons (W. Atwood et al. 2013) detected by the *Fermi*-LAT between 2008 August 5 and 2025 February 2 with an energy range of 0.1-5 GeV photons, from within a 5 deg radius around the radio position of the pulsar. Photon weights were calculated using the `gtsrcprob` routine within `Fermitools` (Fermi Science Support Development Team 2019) and the `P8R3_SOURCE_V3` instrument response functions. These weights correspond to the probability of each photon being associated with the pulsar as opposed to a background source. `gtsrcprob` uses a combination of a spatial model and a spectral flux model using the *Fermi*-LAT 14-year Source Catalog (4FGL-DR4) to calculate the weights (M. Kerr 2011; P. Bruel 2019; S. Abdollahi et al. 2022; J. Ballet et al. 2023).

We used the single photon timing code `event_optimize` within PINT (J. Luo et al. 2019, 2021) to search for pulsations. As a starting point, we searched for any pulsations in the photon data range corresponding to our radio timing baseline (at the time 2.7 yrs) from MJD 59800 to MJD 60800, with no successful detection. This is likely due to the high background confusion given the cluster environment, and proximity to the Galactic plane and bulge.

6. CONCLUSIONS

In this paper, we report the discovery and timing solution of the first pulsar in the GC NGC 6316, PSR J1716–2808A. The system is a 2.45 ms pulsar in

a compact binary system with a $\sim 0.1 M_\odot$ companion. The spin period derivative indicates that unknown combinations of intrinsic spin-down, and accelerations due to the cluster potential, the Galactic potential are impacting our measurement. Continued timing of this pulsar should allow us to measure an orbital period derivative and then disentangle the effects of spin-down and the cluster acceleration (B. J. Prager et al. 2017). However, to constrain cluster properties using accelerations we will need to detect more pulsars within the cluster. Given the mass ($3.5 \times 10^5 M_\odot$ (H. Baumgardt et al. 2023)), the similarities to 47 Tuc, and the number of MSPs estimated via γ -ray spectral analysis (R. de Menezes et al. 2019; W. Wu et al. 2021), we predict that NGC 6316 houses many more MSPs to be discovered. Finding these MSPs will require more sensitive searches, and may be possible using uGMRT, MeerKAT or with the next generation of telescopes, such as the DSA, SKA, or ngVLA.

ACKNOWLEDGEMENTS

The National Radio Astronomy Observatory and Green Bank Observatory are facilities of the U.S. National Science Foundation operated under cooperative agreement by Associated Universities, Inc. Support for this work was provided by the NSF through the Grote Reber Fellowship Program administered by Associated Universities, Inc./National Radio Astronomy Observatory. The Parkes radio telescope (Murriyang) is part of the Australia Telescope National Facility which is funded by the Australian Government for operation as a National Facility managed by CSIRO. We acknowledge the Wiradjuri People as the traditional owners of the Observatory site. We acknowledge the Wallumedegal People of the Darug Nation and the Wurundjeri People of the Kulin Nation as the traditional owners of the land where this work was carried out. SMR is a CIFAR Fellow and is supported by the NSF Physics Frontiers Center award 2020265 and AAG award 2510064.

Facilities: GBT, Parkes, *Fermi*-LAT

Software: PRESTO, PINT, FERMITOOLS, SPIDER_TWISTER

REFERENCES

- Abdo, A. A., Ackermann, M., Ajello, M., et al. 2009, *Science*, 325, 848, doi: [10.1126/science.1176113](https://doi.org/10.1126/science.1176113)
- Abdo, A. A., Ackermann, M., Ajello, M., et al. 2010, *A&A*, 524, A75, doi: [10.1051/0004-6361/201014458](https://doi.org/10.1051/0004-6361/201014458)
- Abdollahi, S., Acero, F., Ackermann, M., et al. 2020, *ApJS*, 247, 33, doi: [10.3847/1538-4365/ab6bcb](https://doi.org/10.3847/1538-4365/ab6bcb)
- Abdollahi, S., Acero, F., Baldini, L., et al. 2022, *ApJS*, 260, 53, doi: [10.3847/1538-4365/ac6751](https://doi.org/10.3847/1538-4365/ac6751)

- Atwood, W., Albert, A., Baldini, L., et al. 2013, arXiv e-prints, arXiv:1303.3514, doi: [10.48550/arXiv.1303.3514](https://doi.org/10.48550/arXiv.1303.3514)
- Ballet, J., Bruel, P., Burnett, T. H., Lott, B., & The Fermi-LAT collaboration. 2023, arXiv e-prints, arXiv:2307.12546, doi: [10.48550/arXiv.2307.12546](https://doi.org/10.48550/arXiv.2307.12546)
- Baumgardt, H., Hénault-Brunet, V., Dickson, N., & Sollima, A. 2023, MNRAS, 521, 3991, doi: [10.1093/mnras/stad631](https://doi.org/10.1093/mnras/stad631)
- Baumgardt, H., Hilker, M., Sollima, A., & Bellini, A. 2019, MNRAS, 482, 5138, doi: [10.1093/mnras/sty2997](https://doi.org/10.1093/mnras/sty2997)
- Bruel, P. 2019, A&A, 622, A108, doi: [10.1051/0004-6361/201834555](https://doi.org/10.1051/0004-6361/201834555)
- Cordes, J. M., & Lazio, T. J. W. 2002, arXiv e-prints, astro, doi: [10.48550/arXiv.astro-ph/0207156](https://doi.org/10.48550/arXiv.astro-ph/0207156)
- Cromartie, H. T., Fonseca, E., Ransom, S. M., et al. 2020, Nature Astronomy, 4, 72, doi: [10.1038/s41550-019-0880-2](https://doi.org/10.1038/s41550-019-0880-2)
- Dai, S., Johnston, S., Kerr, M., et al. 2023, MNRAS, 521, 2616, doi: [10.1093/mnras/stad704](https://doi.org/10.1093/mnras/stad704)
- Davidge, T. J., Harris, W. E., Bridges, T. J., & Hanes, D. A. 1992, ApJS, 81, 251, doi: [10.1086/191692](https://doi.org/10.1086/191692)
- de Menezes, R., Cafardo, F., & Nemmen, R. 2019, MNRAS, 486, 851, doi: [10.1093/mnras/stz898](https://doi.org/10.1093/mnras/stz898)
- Deras, D., Cadelano, M., Ferraro, F. R., Lanzoni, B., & Pallanca, C. 2023, ApJ, 942, 104, doi: [10.3847/1538-4357/aca9ce](https://doi.org/10.3847/1538-4357/aca9ce)
- Fermi Science Support Development Team. 2019, Fermitools: Fermi Science Tools, Astrophysics Source Code Library, record ascl:1905.011 <http://ascl.net/1905.011>
- Freire, P. C. C. 2005, in Astronomical Society of the Pacific Conference Series, Vol. 328, Binary Radio Pulsars, ed. F. A. Rasio & I. H. Stairs, 405, <https://arxiv.org/abs/astro-ph/0404105>
- Freire, P. C. C., Hessels, J. W. T., Nice, D. J., et al. 2005, ApJ, 621, 959, doi: [10.1086/427748](https://doi.org/10.1086/427748)
- Freire, P. C. C., Abdo, A. A., Ajello, M., et al. 2011, Science, 334, 1107, doi: [10.1126/science.1207141](https://doi.org/10.1126/science.1207141)
- Freire, P. C. C., Ridolfi, A., Kramer, M., et al. 2017, MNRAS, 471, 857, doi: [10.1093/mnras/stx1533](https://doi.org/10.1093/mnras/stx1533)
- Fruchter, A. S., & Goss, W. M. 2000, ApJ, 536, 865, doi: [10.1086/308948](https://doi.org/10.1086/308948)
- Hobbs, G., Manchester, R. N., Dunning, A., et al. 2020, Publications of the Astronomical Society of Australia, 37, e012, doi: [10.1017/pasa.2020.2](https://doi.org/10.1017/pasa.2020.2)
- Kerr, M. 2011, ApJ, 732, 38, doi: [10.1088/0004-637X/732/1/38](https://doi.org/10.1088/0004-637X/732/1/38)
- King, I. 1962, AJ, 67, 471, doi: [10.1086/108756](https://doi.org/10.1086/108756)
- Luo, J., Ransom, S., Demorest, P., et al. 2019, PINT: High-precision pulsar timing analysis package, Astrophysics Source Code Library, record ascl:1902.007 <http://ascl.net/1902.007>
- Luo, J., Ransom, S., Demorest, P., et al. 2021, ApJ, 911, 45, doi: [10.3847/1538-4357/abe62f](https://doi.org/10.3847/1538-4357/abe62f)
- Manchester, R. N., Hobbs, G. B., Teoh, A., & Hobbs, M. 2005, The Astronomical Journal, 129, 1993, doi: [10.1086/428488](https://doi.org/10.1086/428488)
- Nice, D. J., & Taylor, J. H. 1995, ApJ, 441, 429, doi: [10.1086/175367](https://doi.org/10.1086/175367)
- Özel, F., & Freire, P. 2016, ARA&A, 54, 401, doi: [10.1146/annurev-astro-081915-023322](https://doi.org/10.1146/annurev-astro-081915-023322)
- Phinney, E. S. 1992, Philosophical Transactions of the Royal Society of London Series A, 341, 39, doi: [10.1098/rsta.1992.0084](https://doi.org/10.1098/rsta.1992.0084)
- Phinney, E. S. 1993, in Astronomical Society of the Pacific Conference Series, Vol. 50, Structure and Dynamics of Globular Clusters, ed. S. G. Djorgovski & G. Meylan, 141
- Prager, B. J., Ransom, S. M., Freire, P. C. C., et al. 2017, ApJ, 845, 148, doi: [10.3847/1538-4357/aa7ed7](https://doi.org/10.3847/1538-4357/aa7ed7)
- Prestage, R. M., Constantinescu, K. T., Hunter, T. R., et al. 2009, IEEE Proceedings, 97, 1382, doi: [10.1109/JPROC.2009.2015467](https://doi.org/10.1109/JPROC.2009.2015467)
- Ransom, S. 2011, PRESTO: Pulsar Exploration and Search Toolkit, Astrophysics Source Code Library, record ascl:1107.017 <http://ascl.net/1107.017>
- Ransom, S. M. 2008, in Dynamical Evolution of Dense Stellar Systems, ed. E. Vesperini, M. Giersz, & A. Sills, Vol. 246, 291–300, doi: [10.1017/S1743921308015810](https://doi.org/10.1017/S1743921308015810)
- Ransom, S. M., Eikenberry, S. S., & Middleditch, J. 2002, AJ, 124, 1788, doi: [10.1086/342285](https://doi.org/10.1086/342285)
- Reid, M. J., Menten, K. M., Brunthaler, A., et al. 2019, ApJ, 885, 131, doi: [10.3847/1538-4357/ab4a11](https://doi.org/10.3847/1538-4357/ab4a11)
- Shklovskii, I. S. 1970, Soviet Ast., 13, 562
- Song, D., Macias, O., Horiuchi, S., Crocker, R. M., & Nataf, D. M. 2021, MNRAS, 507, 5161, doi: [10.1093/mnras/stab2406](https://doi.org/10.1093/mnras/stab2406)
- Verbunt, F., & Freire, P. C. C. 2014, A&A, 561, A11, doi: [10.1051/0004-6361/201321177](https://doi.org/10.1051/0004-6361/201321177)
- Wu, J. H. K., Hui, C. Y., Wu, E. M. H., et al. 2013, ApJ, 765, L47, doi: [10.1088/2041-8205/765/2/L47](https://doi.org/10.1088/2041-8205/765/2/L47)
- Wu, W., Wang, Z., Xing, Y., & Zhang, P. 2021, arXiv e-prints, arXiv:2111.08153, <https://arxiv.org/abs/2111.08153>
- Yao, J. M., Manchester, R. N., & Wang, N. 2017, ApJ, 835, 29, doi: [10.3847/1538-4357/835/1/29](https://doi.org/10.3847/1538-4357/835/1/29)
- Ye, C. S., Kremer, K., Chatterjee, S., Rodriguez, C. L., & Rasio, F. A. 2019, ApJ, 877, 122, doi: [10.3847/1538-4357/ab1b21](https://doi.org/10.3847/1538-4357/ab1b21)

Zhang, C. M., Wang, J., Zhao, Y. H., et al. 2011, *A&A*, 527, A83, doi: [10.1051/0004-6361/201015532](https://doi.org/10.1051/0004-6361/201015532)

Zhang, P., Xing, Y., & Wang, Z. 2022, *The Astrophysical Journal*, 935, L36, doi: [10.3847/2041-8213/ac88bf](https://doi.org/10.3847/2041-8213/ac88bf)